



Elucidating the structural geometry and major faults of the San Marcial Basin, Socorro County, using total Bouguer gravity anomaly data

Kyle K. Gallant, Daniel J. Koning, Andrew P. Jochems, and Alex Rinehart

2022, pp. 341-356. <https://doi.org/10.56577/FFC-72.341>

Supplemental data: <https://nmgs.nmt.edu/repository/index.cfm?rid=2022004>

in:

Socorro Region III, Koning, Daniel J.; Hobbs, Kevin J.; Phillips, Fred M.; Nelson, W. John; Cather, Steven M.; Jakle, Anne C.; Van Der Werff, Brittney, New Mexico Geological Society 72nd Annual Fall Field Conference Guidebook, 426 p. <https://doi.org/10.56577/FFC-72>

This is one of many related papers that were included in the 2022 NMGS Fall Field Conference Guidebook.

Annual NMGS Fall Field Conference Guidebooks

Every fall since 1950, the New Mexico Geological Society (NMGS) has held an annual [Fall Field Conference](#) that explores some region of New Mexico (or surrounding states). Always well attended, these conferences provide a guidebook to participants. Besides detailed road logs, the guidebooks contain many well written, edited, and peer-reviewed geoscience papers. These books have set the national standard for geologic guidebooks and are an essential geologic reference for anyone working in or around New Mexico.

Free Downloads

NMGS has decided to make peer-reviewed papers from our Fall Field Conference guidebooks available for free download. This is in keeping with our mission of promoting interest, research, and cooperation regarding geology in New Mexico. However, guidebook sales represent a significant proportion of our operating budget. Therefore, only *research papers* are available for download. *Road logs*, *mini-papers*, and other selected content are available only in print for recent guidebooks.

Copyright Information

Publications of the New Mexico Geological Society, printed and electronic, are protected by the copyright laws of the United States. No material from the NMGS website, or printed and electronic publications, may be reprinted or redistributed without NMGS permission. Contact us for permission to reprint portions of any of our publications.

One printed copy of any materials from the NMGS website or our print and electronic publications may be made for individual use without our permission. Teachers and students may make unlimited copies for educational use. Any other use of these materials requires explicit permission.

This page is intentionally left blank to maintain order of facing pages.

ELUCIDATING THE STRUCTURAL GEOMETRY AND MAJOR FAULTS OF THE SAN MARCIAL BASIN, SOCORRO COUNTY, USING TOTAL BOUGUER GRAVITY ANOMALY DATA

KYLE K. GALLANT¹, DANIEL J. KONING², ANDREW P. JOCHEMS², AND ALEX RINEHART¹

¹Earth and Environmental Sciences Department, New Mexico Institute of Mining and Technology, 801 Leroy Place, Socorro, NM 87801; kyle.gallant@student.nmt.edu

²New Mexico Bureau of Geology and Mineral Resources, New Mexico Institute of Mining and Technology, 801 Leroy Place, Socorro, NM 87801

ABSTRACT—Gravity surveys are an effective way to aid in interpretation of sedimentary basins, allowing inferences to be made regarding subsurface bedrock depth and geologic structures. A gravity survey was conducted in the San Marcial Basin, Socorro County, New Mexico, over the summer of 2021 in order to clarify the structural geometry and major faults of this basin. The San Marcial Basin was formed as part of the Rio Grande rift, which produced several extensional sedimentary basins from southern Colorado through New Mexico. The topographic basin is covered by a wide blanket of Palomas Formation clastic sediment that is minimally faulted, so field mapping only gave hints of the basin's structural geometry and potential major geologic structures. In this study, 89 new gravity measurements were tied to National Geospatial-Intelligence Agency (NGA) benchmarks. At each location, gravity and GPS measurements were taken, with GPS coordinates measured to a resolution of 5 cm vertical and horizontal. Interpreting the processed data indicates a 10–20 km wide region of deeper basin fill (widening to the north) centered near the axial river of the rift, the Rio Grande. A 3–5 km wide arm of deep basin fill extends north-eastward under Mesa del Contadero. There is weaker evidence for two gravity-low, embayment-like features that extend northward from the wider gravity-low centered on the Rio Grande. One of these gravity-low embayments extends northwards ~5 km between the southern Chupadera Mountains and southern Magdalena Mountains, corresponding to the southernmost Highland Springs topographic embayment, and the other appears to approximately follow NM State Road 107 for ~15 km northwest of its intersection with Interstate 25 (I-25). Analyzing the processed data also indicates two notable, linear, total Bouguer gravity anomalies in the south-central and eastern part of the basin. The western anomaly is correlated to the down-to-the-east Black Hill fault, which strikes NW and forms fault scarps on select middle Pleistocene surfaces. The eastern anomaly is a pronounced west-down gravity gradient that strikes NNE, which we interpret as a west-down fault. This eastern anomaly, here named the Lava fault, coincides with a laid-back escarpment east of the Rio Grande. The Bison Corral well in the footwall of the fault and the subsurface stratigraphy of the Pope boring within the Lava fault zone, indicate shallow Cretaceous bedrock (15 m in the Bison Corral well) east of the Lava fault, providing support that this eastern gradient is due to vertical displacement of bedrock rather than juxtaposition of two different bedrock types. The Lava fault projects southwards to a location about 5 km east of the northern end of the Fra Cristobal Mountains, separating the shallow Cretaceous bedrock from a gravity low immediately east of the north end of the Fra Cristobal Mountains; more data are needed to constrain the location of the Lava fault in that area. The lack of noteworthy footwall uplifts along either the Black Hill or Lava faults, especially when compared to the prominent Fra Cristobal Mountain footwall uplift on the Walnut Springs fault to the south, may possibly be due to a northward partitioning of extensional strain from the Walnut Springs fault to the Black Hill and Lava faults. In this hypothesis, which remains to be tested by numeric modeling, lowered vertical displacement rates on either fault resulted in low footwall uplift rates that could not outpace long-term erosion rates or burial by sedimentation.

INTRODUCTION

Gravity surveys measure the acceleration of the Earth's gravity field in select locations and are sensitive to variations in subsurface density. Spatial variations in density in sedimentary basins can be used to map basin structure, with lower measured values being associated with less dense material. Gravity data are commonly presented as gravity anomalies, which is the difference between measured gravity values and expected values if the Earth was an ideal oblate spheroid composed *entirely* of bedrock of uniform density. Contrasts in density can occur within the bedrock of the crust, but commonly the greatest density contrasts occur between weakly to moderately consolidated, weakly cemented basin fill versus generic bedrock. Deeper (thicker) basin fill has a relatively lower density, even at depth, compared to bedrock and would be expected to produce a relatively lower gravity signal. In a geophysical study

to the north in a Rio Grande rift basin (Grauch et al., 2009), the basin fill (Santa Fe Group) was shown to be considerably less dense than other rock types (with differences >140 kg/m³). A gravity survey with sufficiently close-spaced stations can elucidate areas of lower gravity anomalies—corresponding to lower density compared to *all* bedrock types—that may correspond to areas of thicker basin fill. These surveys may also demarcate sharp gradients in the gravity anomaly that may be interpreted as fault lines juxtaposing thicker basin fill with shallower basin fill. Gravity surveys have previously been used to great effect to understand many of the larger sedimentary basins of the Rio Grande rift (Adams and Keller, 1994; Grauch et al., 2009; Grauch and Connell, 2013; Grauch et al., 2017; Drenth et al., 2019).

This study collected 89 new gravity measurements in the topographic San Marcial Basin, weakly consolidated in the south-central Rio Grande rift (Fig. 1). We synthesize these

data with historic gravity data and recent geologic mapping to interpret the general geometry of this basin and major geologic structures. Other than a focused geophysical effort to determine and understand the geologic causes of a fissure in the northern topographic San Marcial Basin (Haneberg et al., 1991), this basin has received little previous attention. Only in recent years has 1:24,000 geologic mapping been conducted (Jochems and Koning, 2019; Koning et al., 2020a, b, 2021). This mapping indicated that only young rift fill is exposed, the Plio-Pleistocene Palomas Formation of the Santa Fe Group,

and these strata are minimally tilted and faulted. Many geomorphic surfaces have developed on the Palomas Formation, the highest and oldest projecting approximately to the base of the 818.3 ± 10.6 ka basalts on Mesa del Contadero (Fig. 3; represented as QTb; Koning et al., 2020a, 2021; age of basalt from Sion et al., 2020). The relative paucity of surface expression of faults in the topographic San Marcial Basin underscored the need to employ geophysical methods such as gravity to better understand the basin geometry and major structures. In the following, the term “San Marcial Basin” is used in a

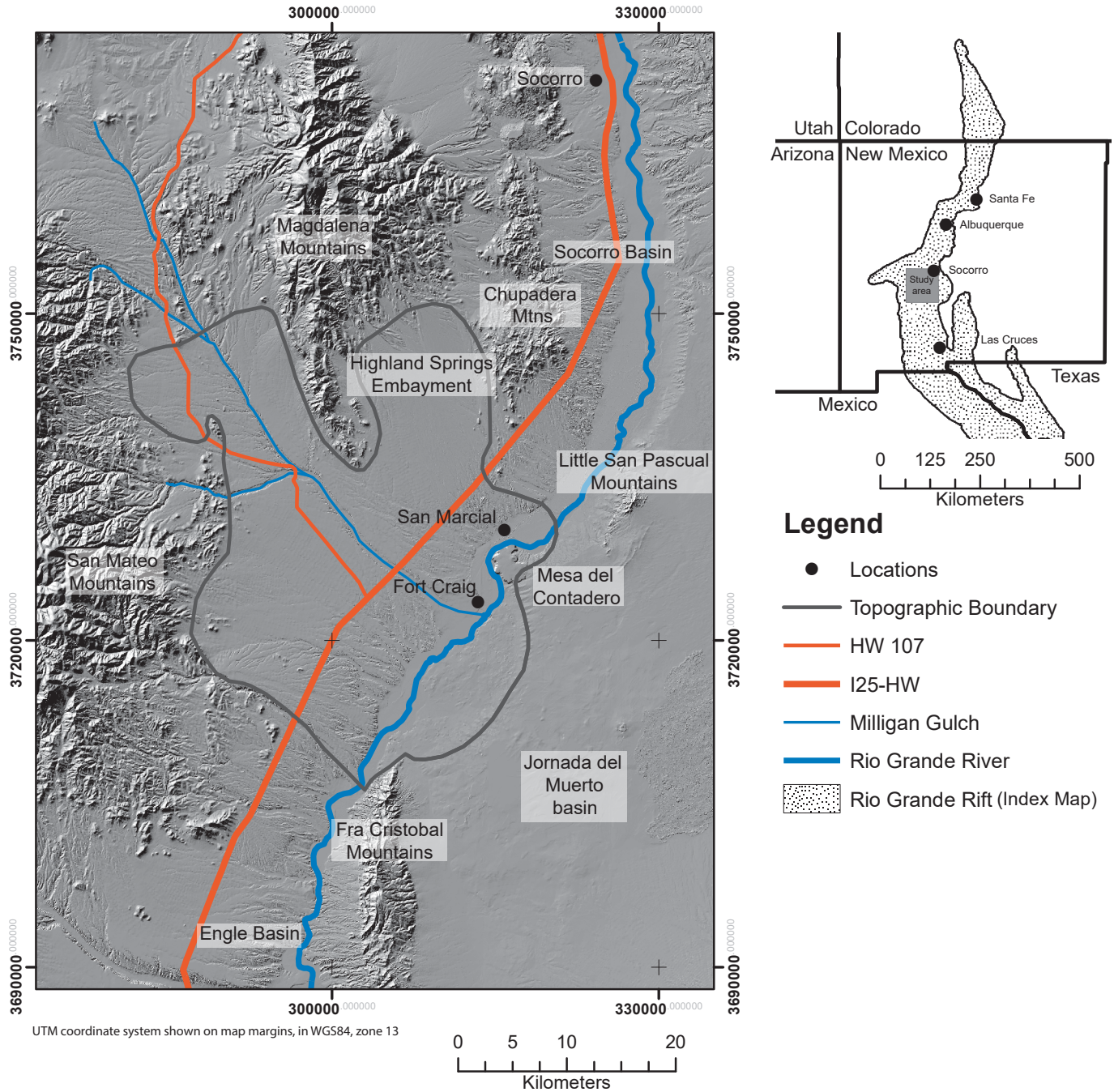


FIGURE 1. Geographic setting of the San Marcial Basin, relative to adjoining geographic features. Index map in the upper right shows the location of study area, in gray shade, relative to the state of New Mexico. The topographic San Marcial Basin is bounded by mountains and hills on the north, west, and south; on the east it is bounded by a 60 m (200 ft) tall escarpment formed by the basalt in the Jornada del Muerto Basin. Northing and Eastings are labeled on the map margins (WGS84, zone 13).



FIGURE 2. Photograph looking north toward Mesa del Contadero (right) and the Chupadera Mountains (central skyline) across the northern San Marcial Basin. The northern San Mateo Mountains are located on the left skyline. Mesa del Contadero is a prominent landmark in the San Marcial Basin.

structural sense; where used as a geographic term, the adjective “topographic” is added (e.g., “topographic San Marcial Basin”). It should be noted that basin boundaries shown in all figures are of the topographic San Marcial Basin (e.g., Fig. 3).

SETTING

Tectonic Setting in Rio Grande Rift

The San Marcial Basin is an extensional sedimentary basin in the Rio Grande rift of central New Mexico. It lies between the Socorro Basin to the north and the Engle Basin to the south (Fig. 1). The Rio Grande rift is a north-trending, intracontinental rift feature caused by extensional tectonic activity thought to have begun about 26 Ma (Chapin 1979; Chapin and Cather, 1994). The basins step rightwards along a N-S trend and generally consist of asymmetric half grabens. Examples of asymmetric basins include the northern San Luis Basin (Kluth and Schaftenaar, 1994), eastern Española Basin (Biehler et al., 1991; Koning et al., 2013), Calabacillas sub-basin of the Albuquerque Basin (Connell, 2008; Connell et al., 2013; Grauch and Connell, 2013), and Palomas Basin (Gilmer et al., 1986).

Geographic Features of the Topographic San Marcial Basin

The topographic San Marcial Basin is small to medium in size, compared to other rift basins, and named after an abandoned historical town (Fig. 1). The maximum dimensions of the topographic San Marcial Basin are ~43 km (N-S) and ~33 km (E-W). The Rio Grande flows south across the eastern part of the topographic basin. The only major tributary to the Rio Grande in the basin is Milligan Gulch, which flows southeast into the Rio Grande and is southwest of Mesa del Contadero (Figs. 1, 3).

Topographically high areas bound the San Marcial Basin (Fig. 1). To the north of the basin are the Chupadera and Magdalena Mountains (Fig. 1). The San Mateo Mountains flank the western portion of the basin. The San Mateo and Magdalena

Mountains are generally 2900 m (9500 ft) in elevation, while the Chupadera Mountains are much lower at 1710 m (5600 ft). To the east of the San Marcial Basin is a broad, partially basalt-capped mesa comprising the minimally dissected, northern part of the Jornada del Muerto Basin. The geomorphic surface of the Jornada del Muerto Basin projects to the base of basalts capping Mesa del Contadero (Fig. 2). The southern end of the San Marcial Basin corresponds to the northern extent of two mountainous areas: the northern Fra Cristobal Mountains and unnamed hills extending eastward from the southern end of the San Mateo Mountains (Fig. 1). The surface of the topographic San Marcial Basin ranges from 1340 m (4400 ft) in the Rio Grande floodplain to 1980 m (6500 ft) at the eastern front of the San Mateo Mountains. There are two topographic embayments in the northern topographic San Marcial Basin. One embayment extends northwest along Milligan Gulch, and the other, informally called the Highland Springs embayment, is situated between the southern Magdalena Mountains and the southern Chupadera Mountains (Fig. 1).

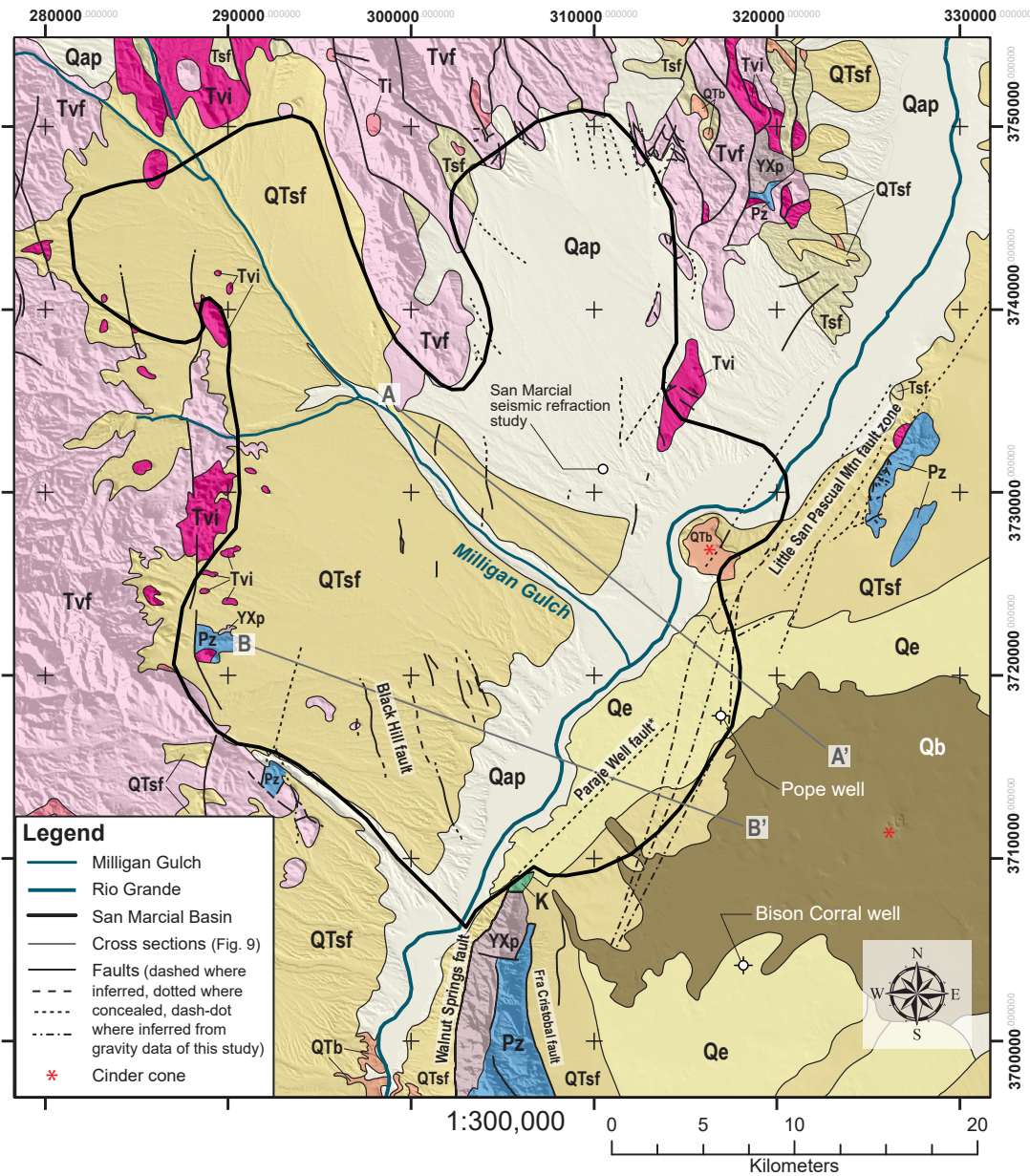
Geology of the San Marcial Basin

Away from the mountains, only a few bedrock hills are present in the San Marcial Basin on its southwest side, mainly composed of late Eocene–early Oligocene volcanic rocks and Pennsylvanian sedimentary strata with minor Proterozoic rocks (Fig. 3). Otherwise, the San Marcial Basin is underlain by a wide blanket of clastic detritus (sand, gravel, silt, clay) mapped as the Palomas Formation of the Santa Fe Group (Fig. 3), which is Pliocene to early Pleistocene in age (Jochems and Koning, 2019; Koning et al., 2020a, b, 2021; Morgan et al., this volume). Underlying the Palomas Formation is an unknown thickness of Miocene strata correlated to the Popotosa Formation (e.g., cross sections of Koning et al., 2020a, b, 2021).

There is a paucity of well and geophysical data in the San Marcial Basin, but what is available can be used to constrain our gravity interpretations. The deepest wells, having 94–140 m (310–460 ft) depths, are found in and near Milligan Gulch about 1–4 km northwest of I-25 (Koning et al., 2021, ArcMap geodatabase). Based on interpretation of driller logs filed with the New Mexico Office of the State Engineer, these wells penetrated conglomerates and sandstones of the Santa Fe Group. A seismic refraction study at the San Marcial fissure site (Fig. 3) indicated a top-of-bedrock depth of 80 m (260 ft; Haneberg et al., 1991). The Pope borehole on the east side of the basin is 122 m (400 ft) deep and is entirely in the Palomas Formation (Figs. 3, 4). At a depth of 107–115 m (350–380 ft) is a tongue of distinctive, locally derived gravel composed of greenish sandstone clasts, correlated sandstones in the Cretaceous Crevasse Canyon Formation, and minor gray limestone (Fig. 4). Above and below this locally derived gravel lies axial-fluvial sand of the ancestral Rio Grande. On the southeast side of the study area, 13 km due-east of the north end of the Fra Cristobal Mountains, lies the Bison Corral well (Fig. 3; Appendix 1). The Bison Corral well was drilled to a depth of 84 m (275 ft). Weakly consolidated, silt, clay, and sand correlated to the Palomas Formation (Santa Fe Group) is 15 m (50 ft) thick.

Below is Cretaceous strata, based on the presence of gray-yellow clays and silts, local descriptions of “oil shale,” lack of limestone beds, and lack of conglomerates. The shallow bedrock at this well is an important consideration in our gravity study and is interpreted to be comprised of Gallup Sandstone, D Cross Tongue of Mancos Shale, and Tres Hermanos Formation (descending stratigraphic order).

Several named faults have been previously mapped in and near the San Marcial Basin (the Paraje Well, Little San Pascual Mountain, Black Hill, Fra Cristobal, and Walnut Springs faults; Fig. 3). The Walnut Springs fault that bounds the 25 km long, western front of the 500 m tall Fra Cristobal Mountains (Fig. 3) was referred to as the Hot Springs fault by Nelson et al. (2012), and it defines the eastern boundary of the Engle Basin,



Lithologic Units

Quaternary	Neogene-Quaternary	Eocene-Oligocene	Older rocks
Qe Eolian sand	QTsf Upper Santa Fe Group	Tvf Felsic volcanics	K Cretaceous sedimentary
Qap Valley-floor or piedmont alluvium	QTb Miocene-Pliocene basalt	Tvi Intermediate volcanics	Pz Paleozoic sedimentary
Qb Basalt (~820 ka)	Tsf Santa Fe Group	Ti Intrusive rocks	YXp Precambrian plutonic

FIGURE 3. Simplified geologic map based on the 1:500,000 statewide geologic map of New Mexico (NMBGMR, 2003). Note that the Paraje Well fault of Koning et al. (2020b) is shown for reference, but as a result of our study we now interpret that there is no evidence to support its existence.

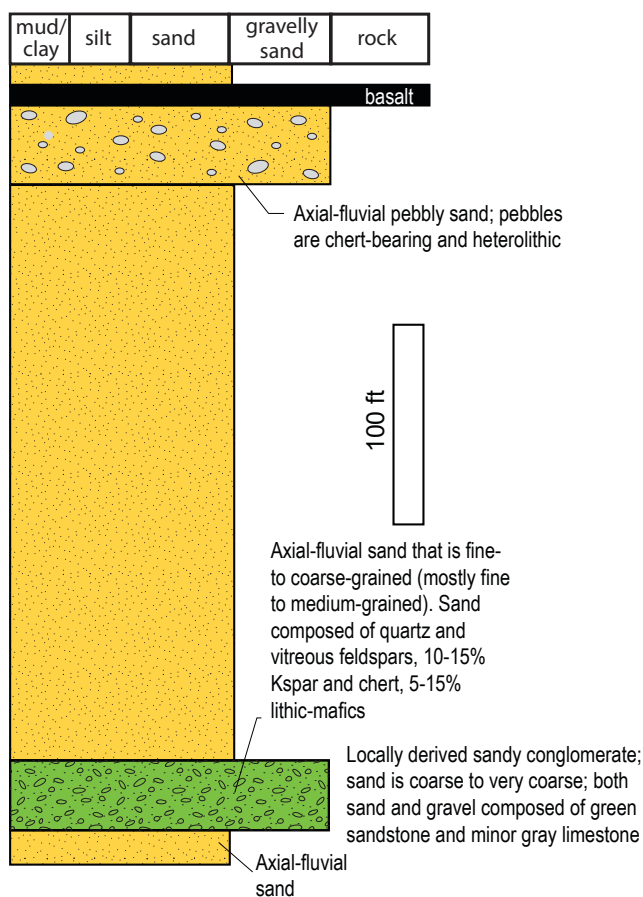


FIGURE 4. Graphic column and description of subsurface stratigraphy for the Pope borehole, drilled on January 27–28, 2022. Location is 316,945 m E, 3,717,765 m N (NAD83, zone 13). The presence of a layer of locally derived conglomerate at 107–116 m (350–380 ft) depth, composed of greenish sandstone and minor gray limestone, is interpreted to indicate relatively shallow bedrock to the east underlain by a large extent of Crevasse Canyon Formation (Kelley and Koning, this volume). The interpreted presence of Crevasse Canyon Formation to the east would imply that rift-related, extensional strain of the Lava fault zone reactivated an earlier west-side up, west-dipping Laramide fault system, probably a northward continuation (albeit offset by younger extensional faults) of the reverse fault mapped in the northern Fra Cristobal Mountains (Nelson et al., 2012).

the next basin south of the San Marcial Basin (Fig. 1). This fault likely has much greater throw (Machette, 1987) than the ~1 km shown for the Hot Springs fault in the southern Engle Basin (Lozinsky, 1987), which links northward with the Walnut Springs fault (south of area shown in Fig. 3). The amount and timing of Quaternary motion on this fault is uncertain (Machette and Jochems, 2016a). On the east side of the Fra Cristobal Mountains is the east-down Fra Cristobal fault (Nelson, 1986). The concealed Paraje Well fault mapped by Koning (2020b) was assumed to continue northeastward from the Walnut Springs fault (Fig. 3), but no direct evidence for it was found in that mapping effort. The Little San Pascual fault system is a west-down structure that is found within 2 km of the western front of the Little San Pascual Mountains (Koning et al., 2020a; Koning, this volume). South of the mountains, the locations and existence of its three main strands are uncertain. The Black Hill fault is demarcated by two northwest-striking (330°), northeast-down fault scarps located 1–10 km west of

the Rio Grande (Fig. 3) and separated by a distance of 2.5 km. These faults have produced <5 m tall fault scarps on select geomorphic surfaces developed in early and middle Pleistocene deposits (Machette and Jochems, 2016b; Jochems and Koning, 2019). On the southwest side of the western fault, scattered hills of late Eocene to early Oligocene volcanic bedrock are present (Fig. 3; Jochems and Koning, 2019). At the initiation of this study, we hypothesized that the Paraje Well, Black Hill, and possibly the southern extension of the Little San Pascual Mountain faults exhibited sufficient vertical displacement as to control the structural geometry of the basin.

METHODS

The survey we conducted covered an area of roughly 870 km² and two new absolute stations and 89 new relative gravity stations (Fig. 5). The duration of the survey was three weeks in July of 2021.

Field Methods

The majority of the basin was surveyed at a 1.25 km to 1.75 km spacing, including pre-existing stations. Several areas had denser networks deployed to answer structural questions raised by pre-existing mapping. Two new absolute gravity locations (smb_west_aa, and smb_east_aa; Fig. 5) were established in the central basin on either side of the Rio Grande to provide reference stations for the network (R.D. Wheeler, pers. commun., 2021).

Gravity measurements and GPS location measurements were taken in tandem using a ZLS Burris Calibrated Screw-type Gravity Meter (S/N B107) and a Trimble RTX GPS system (S/N 5250K40787) with a Trimble NetR9 receiver, Zephyr 2 Geodetic antenna, and TSC3 handheld. Measurements would start and end every day at an absolute gravity location. During each day, a subset of stations were re-occupied every ~90 minutes; the survey was performed using local loops, with approximately 1/3 of the stations being occupied more than once. Ten of the 89 relative stations were subsequently tied to the absolute reference stations with at least three reoccupations; these ‘tied’ stations were chosen from the stations reoccupied during the local loops to minimize uncertainty.

Each relative station was a 30 x 30 cm paver that was placed and roughly leveled on the ground (Fig. 6). The GPS antenna bipod with the antenna at 2 m height was placed on the southwestern corner of the paver first, then the gravimeter was placed on the northern half, so measurements could be made simultaneously (Fig. 6). Pavers were removed after the survey. During the survey, one of the leveling tripod meter legs was kept at a fixed position so that all meter heights were consistent throughout the survey to within a few mm.

Measurements were taken over at least two minutes, collecting 10 second moving average relative gravity measurements every 5 seconds while monitoring the standard deviation and beam error of the meter. If standard deviations exceed ~30 μ Gal, then more measurements were collected, for up to 5 minutes of data. Additionally, we monitored for trends during the

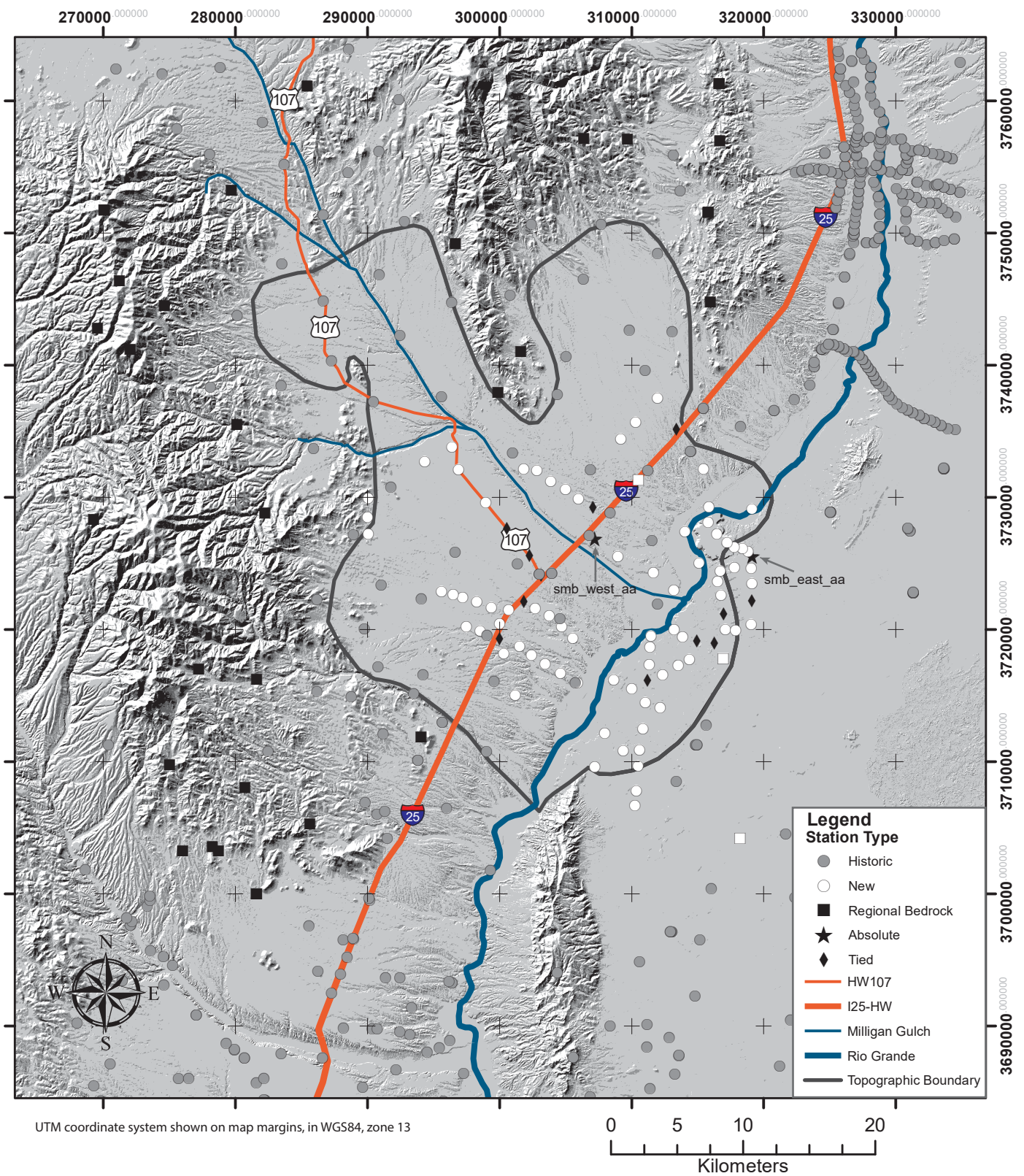


FIGURE 5. Map showing locations of gravity data in the topographic San Marcial Basin. Topographic basin boundary is shown as a black line. Relative gravity stations collected during this study (white circle and black diamond), historical relative gravity stations (gray circle and black box) used in this study, and newly collected absolute gravity stations (star) are shown. ‘Tied’ stations are relative stations with at least three loops to an absolute station. Regional bedrock stations were used to remove the regional crustal gravity trend.



FIGURE 6. Instrument setup used during the survey, with the gravimeter (small gray box on the left of the paver) pointing to the north and the GPS system planted on the southwest corner. Mesa del Contadero is on the right. To the left of the mesa is the site of the 1862 Battle of Valverde, the largest Civil War battle in the western United States (Koning, this volume).

measurements, which might indicate the meter shifting from level or the arrival of seismic waves from earthquakes; if such a trend occurred, the measurements were retaken until they stabilized. In the case of earthquakes, the nearest loop base station would be reoccupied after the vibrations quieted to background levels, and then the loop would be redone.

Significant elevation and subsurface density changes occurred within the extent of the survey, necessitating changing the ‘dial’ or effective calibrated range of the meter. When this happened, we found a location where measurements for both dial settings were possible and measured the relative gravity at both settings; these stations were also used as ties to the absolute base stations, if possible. This was generally within survey uncertainty (0.015 mGals) but was still corrected similar to a tare.

Four RTX GPS location measurements were taken at 15 second intervals with a requirement of better than 3 cm horizontal accuracy and 5 cm vertical accuracy. Differential corrections were provided by the RTX service, and the accuracies were reported by the Trimble software. Locations were recorded in decimal degrees in the ITRF2014 reference frame. During post-processing, these were re-projected to UTM Zone 13N WGS84. Projection errors were within the uncertainty of the measurements and less than the maximum error in location needed to interpret the gravity data.

Historical data were compared to new data, where possible, and had new terrain corrections applied to them (see below). Additionally, historical data were reviewed for outliers; only two points were found to be more than 1–2 mGals off of expected trends, and overall the newly terrain-corrected Bouguer anomalies of historical data fit within the trends of the newly acquired, higher quality data. We recognize that there often are significant errors associated with the historical data. However, data overall in the region were sparse, and we found, overall, that the magnitude and spatial trends in historical data were consistent with our higher-resolution survey.

Data Reduction

All raw gravity and location time series were averaged after removing any high standard deviation or erroneous measurements. All of the data was then segmented by day. Within each day, drift rates were calculated between every pair of reoccupations; erroneously high drift rates were interpreted as tares and the affected instrument measurements were corrected. After a single tare was corrected and dial change offsets were corrected similarly to tares (tares being static offsets in the data that cannot be attributed to general variations, or drift, that can occur during surveys), the remaining drift rates were manually reviewed. Drift rates were low ($<10 \mu\text{Gal}/\text{hour}$, often less than $5 \mu\text{Gal}/\text{hour}$) and were consistent over each day. We used the daily drift rate to correct the data after ensuring that higher-resolution drift rates were consistent with the daily drift rate.

The free air anomaly was already calculated for historical data but needed to be obtained for our new measurements. The gravimeter controller software made tidal corrections using Longman (1959) during the survey after the latitude, longitude, and elevation of each station were entered. Latitudinal and meter height corrections were made, and atmospheric corrections were neglected (Hinze et al., 2013). Then the free-air anomaly was calculated using Hinze et al. (2013). Bouguer gravity anomaly was calculated from the free air anomalies using Hirt et al. (2019), assuming a rock density of $2.67 \text{ g}/\text{cm}^3$.

We observed a regional, roughly planar trend in the terrain-corrected Bouguer values that dipped to the northwest. We believe that this trend is due to underlying bedrock or crustal density variations, rather than variations in basin fill thickness (Hinze et al., 2013). Thirty-three stations on bedrock were identified. Using their locations (UTM, zone 13N) and total Bouguer anomaly values, we fit a planar surface to their total Bouguer anomaly values using a least-squares regression in Matlab ($R^2 = 0.945$, residual mean of 10^{-13} mGal, standard deviation of 4.173 mGal, maximum absolute residual of 9.401 mGal). All bedrock stations are west of the Rio Grande and north of the Fra Cristobal Mountains (Fig. 6); residuals from the Rio Grande east are extrapolations. We applied second and third order polynomial fits as well, without significantly increasing the goodness of fit; to avoid overfitting, we chose the planar model. Data were too sparse for more sophisticated harmonic trend removal or edge detection. We removed the modeled bedrock total Bouguer gravity anomaly trend for every gravity station to find a residual anomaly that should be more

sensitive to bedrock topography (Hinze et al., 2013).

To aid interpretation, we interpolated the total Bouguer anomaly and residual anomaly using inverse distance weighting (IDW) in the ArcGIS Spatial Analyst toolbox. The default values for IDW were used (12 neighbors, no limit on distance). We chose a 150 m grid size for the interpolation grids.

RESULTS

General Basin Geometry

Figures 7 and 8 show maps of the total Bouguer gravity anomaly and residual anomaly, respectively, for the San Marcial Basin relative to mapped and inferred faults. In regards to the confidence of the residual anomaly gravity data, shallow basin fill thicknesses near the Bison Corral well and east of the Pope borehole, the latter inferred using the locally derived gravel tongue at 107–116 m (350–380 ft) depth (Fig. 4), supports our interpretations that near-zero residual gravity anomalies east of the Rio Grande (Fig. 8) correspond to little to no basin fill. This region has no other bedrock control, so the plane fit to the regional trend is extrapolated here. The residual gravity between the Pope borehole and Bison Corral well is generally not as reliable as to the west, both because of the lack of bedrock stations and because of the lack of any new gravity stations (Figs. 6–8). West of the river, the refraction survey supports the interpretation of minimal basin fill for residual gravities near 0 mGal and greater (Fig. 8). The relatively low residuals interpolated near the seismic refraction study at the San Marcial fissure site (-3 to -7 mGals) are consistent with the 80 m bedrock depth there (Haneberg et al., 1991).

Two cross sections (Fig. 9) were created by integrating geologic map data (Jochems and Koning, 2019; Koning et al., 2020a, b, 2021) with the gravity maps. Cross section lines follow A-A' and B-B' on Figures 3, 7, and 8. To aid in basin fill thickness (i.e., top of bedrock elevation), profiles were constructed of total Bouguer and residual anomaly gravity data, where values were projected orthogonally onto the two section lines, and using these gravity data we adjusted the bedrock top in a qualitative manner. From these maps and cross sections, several general observations can be made regarding the structure and extent of the basin.

South-central, Broad (Main) Gravity Low

In the south-central portion of the basin, there is a broad gravity low extending between the Lava and Black Hill faults (Lava fault labeled in Figs. 7–9 and described below). This area of low Bouguer anomalies and residual anomalies is found within 5–10 km of the Rio Grande, being slightly lower west of the river in both the total Bouguer anomaly and residual datasets (Figs. 7–9). Compared to the total Bouguer anomaly (Fig. 7), when the bedrock trend surface is removed, the residual anomaly of the south-central part of the study area appears deeper, broader, and exhibits a slightly higher gradient along its southeastern boundary (Fig. 8). We do not interpret the structural transition (or boundary) between the San Marcial

and Engle Basins because that area on the maps, west of the north end of the Fra Cristobal Mountains, reflects an interpolation rather than data.

The broad gravity low in the south-central part of the study area is interpreted as reflecting thickened basin fill, corresponding to where the bedrock floor has subsided most. The interpretation of thickened basin fill is consistent with the lack of bedrock outcrops in this area. In addition, the well control of Koning et al. (2020b, 2021) indicate minimum Santa Fe Group thicknesses of 94–140 m (310–460 ft) in the northeast end of this broad gravity low, at a location 1–4 km northwest of the intersection of Milligan Gulch and I-25. Residual anomalies are even lower 5–10 km to the south of that location, suggestive of even greater basin fill thickness. In contrast, bedrock is only 15 m (50 ft) deep near the Bison Corral well, where the total Bouguer anomaly is notably higher (based on five historic gravity stations) than near the Rio Grande (Fig. 7).

One alternative cause of the low Bouguer anomalies in the south-central San Marcial Basin (Fig. 7) could be low-density plutons. However, when we de-trend the regional crustal Bouguer anomaly—including stations near the Oligocene calderas in the northwestern corner of the study area (Fig. 7)—we find that the residual gravity anomalies in the south-central San Marcial Basin are -20 to -33 mGals (Fig. 8). In addition to the well control listed above, this notably low residual anomaly implies that the south-central observed low anomalies are not associated with regional crustal density trends, such as intrusion of low-density plutons.

Northwestern Study Area

In the total Bouguer anomaly map, low gravity values characterize the northwest corner of the study area, especially west of the Magdalena Mountains (Fig. 7). After removing the regional bedrock trend, the residual anomalies show values consistent with bedrock being near the surface (>0 mGal residual) rather than being caused by basin fill (Fig. 8). This area could be undergirded by low-density plutons. In particular, the 27.6 Ma Mount Withington caldera (Fig. 7), located west and northwest of the northwest corner of the topographic basin, has been well studied and is interpreted to contain 700 km³ of felsic tuff that is ~1 km thick (Deal, 1973; Donze, 1980; Deal and Rhodes, 1976; Ferguson, 1986, 1990, 1991; Ferguson and Osburn, 1994; Ferguson et al., 2012). A relatively large, felsic pluton under that caldera would not be unexpected. Another felsic pluton may exist under the Hardy Ridge caldera (Fig. 7), located between Milligan Gulch and the central Magdalena Mountains (Ferguson et al., 2012). The coincidence of some of these calderas, particularly the Mt. Withington caldera, with low total Bouguer anomaly values (Fig. 7) but positive residual anomalies (Fig. 8), supports the inference that crustal pluton may be responsible for the W-NW-decreasing crustal density trend in the total Bouguer anomaly data (Fig. 7). Shallow plutons away from these interpreted calderas would be less likely, but cannot be ruled out.

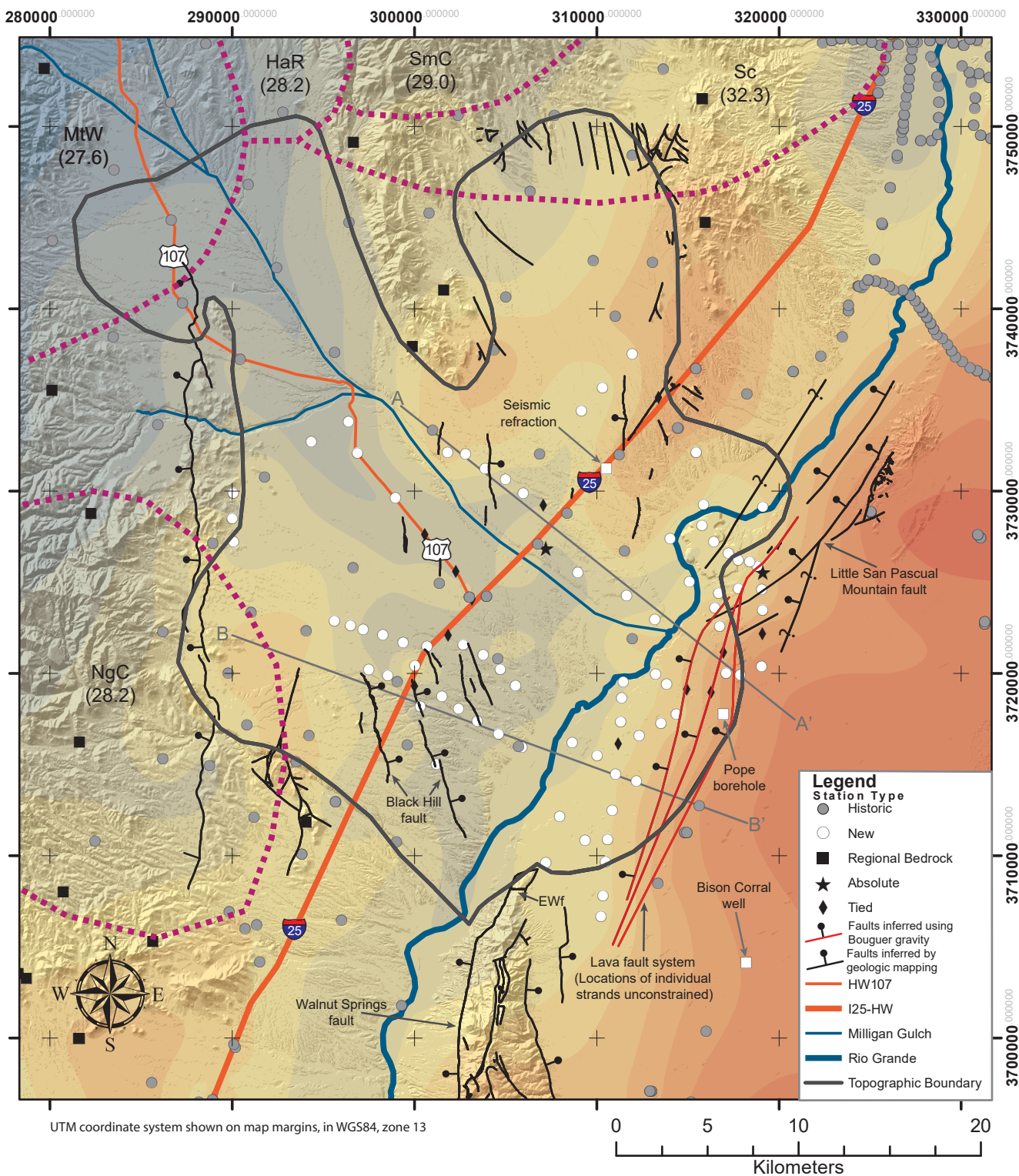


FIGURE 7. Map showing total Bouguer anomaly gravity data, included inferred faulting locations. Also displayed are boundaries of Oligocene calderas (modified after Chamberlin et al., 2004) and their ages (Ma) around the northern and western portions of the basin. Abbreviations of caldera names are displayed in the figure. NgC – Nogal Canyon caldera (28.7 Ma), MtW – Mount Withington caldera (27.6 Ma), HaR – Hardy Ridge caldera (28.2 Ma), SmC – Sawmill Canyon caldera (29.0 Ma), Sc – Socorro caldera (32.3 Ma).

Embayments

There are three embayment-like, Bouguer anomaly lows that extend northeast, north, and northwest from the main, broad Bouguer anomaly low in the south-central part of the San Marcial Basin. Like the main Bouguer low to the south, we infer these embayment-like gravity lows also reflect thickened basin fill (Fig. 8). This is consistent with their spatial coincidence in topographically lower areas, the presence of 310–460 ft deep wells in Milligan Gulch located 1–4 km northwest of I-25 that did not encounter bedrock (Koning et al., 2021, cross sections), and the lack of bedrock outcrops in those areas. Additionally, the residual values show a similar geometry (Fig. 8) as the total Bouguer anomaly (Fig. 7), which gives us confidence that these features represent areas of thickened basin fill.

Southeast of the southern Chupadera Mountains, a 3–5 km wide low extends >10 km northeast under the Rio Grande and Mesa del Contadero. Its southern part is well constrained by a relatively dense network of gravity stations (Figs. 7, 8), but its northeast end is poorly constrained. The extension of this low to the northeast toward the Socorro Basin becomes larger in the residual anomaly map than in the total Bouguer anomaly map (Figs. 7, 8). The residual gravity anomaly in this northeast-trending embayment is similar to that found in the main, south-central low, suggesting similar basin fill thicknesses. In the residual anomaly data, the southeastward prong extending south of the Little San Pascual Mountains appears to be an interpolation artifact from a lack of data east of our network (Fig. 8).

West of the south end of the Chupadera Mountains, a negative gravity anomaly underlies the southernmost end of the Highland Springs topographic embayment. This particular Bouguer anomaly low is bounded to the northwest by the southern end of the Magdalena Mountains, on the north by a ridge-like, northwest-trending gravity high (which may be an artifact of sparse historical gravity data), and on the east-northeast by the southern Chupadera Hills (Fig. 7). There is a 5 mGal decrease of the residual gravity data in the southernmost Highland Springs embayment compared to the seismic refraction study at the San Marcial fissure site, but there is a bigger drop in the residual anomaly (15 mGals) between the southernmost embayment and the main, south-central Bouguer anomaly low to the south. Given that the basin fill depth at the seismic refraction site is 80 m (Hananberg et al., 1991), the southernmost Highland Springs embayment could possibly be ~100 m depth, whereas the main gravity-low to the south is likely deeper than 100 m, consistent with the 94–140 m (310–460 ft) minimum Santa Fe Group thickness near 1–4 km northwest of the intersection of Milligan Gulch and I-25.

To the southwest of the Highland Springs embayment, in the aforementioned topographic embayment between the southern Magdalena Mountains and the San Mateo Mountains, there appears to be a northwest-trending gravity low in both the total Bouguer anomaly and residual anomaly maps near NM State Route 107, paralleling and a few kilometers south of Milligan Gulch (Figs. 7, 8). Within 15 km northwest of I-25, residual anomalies are relatively comparable to those found in the

Highland Springs topographic embayment. Beyond 15 km to the northwest, the residual anomalies are lower (Fig. 8) based solely on analysis of historical data, suggestive of comparably thin basin fill in most of the topographic embayment between the San Mateo and Magdalena Mountains. This area has few gravity stations and notable uncertainty exists.

Bouguer Anomaly Highs

With the exception of the San Mateo and Magdalena Mountains, higher total Bouguer gravity anomalies mostly correspond to areas with exposed bedrock (Figs. 3, 7) and have near-zero or positive residual anomalies (Fig. 8). In the southwestern part of the basin, relatively high Bouguer and residual anomalies are present west of I-25 and northeast of the low hills extending southeastward from the southern San Mateo Mountains (Figs. 7, 8). In this area, there are scattered bedrock hills composed of Pennsylvanian sedimentary rocks and late Eocene–early Oligocene volcanic rocks (Fig. 3; Jochems and Koning, 2019). A relatively high Bouguer and residual anomaly also exists in the central and northern Highlands Springs topographic embayment, and slightly higher values spatially correspond to the exposed volcanic bedrock of the Chupadera Mountains (Figs. 7, 8; Koning et al., 2020; Cikoski et al., 2013). Based on five historical gravity data stations, there is a prominent positive anomaly near the western part of the mesa located east of the Rio Grande, near the southeastern end of cross section B-B' (Figs. 7, 8). This positive anomaly appears to extend southwards past the Bison Corral well and 20–30 km to the northeast, based on historical gravity data. Note that this eastern area is away from any bedrock control points for the residual anomaly, and the total Bouguer anomaly should be given priority of interpretation.

Faults

Gradients in Bouguer and residual anomaly gravity data indicate lateral juxtaposition of lithologic materials of different densities. Where linear and particularly pronounced, these gradients are suggestive of faults juxtaposing thick basin fill against bedrock, particularly since basin fill densities are notably less than those of various bedrock types (e.g., Grauch et al., 2009). However, there could still be faults where there are no such gradients, particularly where the juxtaposed sediment or rock types have similar densities (e.g., low- to moderate-displacement, intra-basin faults or faults juxtaposing bedrocks of similar densities). We interpret that two Bouguer and residual gravity anomaly gradients, found on either side of the aforementioned gravity low in the south-central San Marcial Basin (centered on the Rio Grande), are due to normal faulting that juxtaposed thick basin fill against shallow bedrock. We interpret that the western of these gradients correlates to the Black Hill fault, and the eastern correlates to a fault we elect to call the Lava fault.

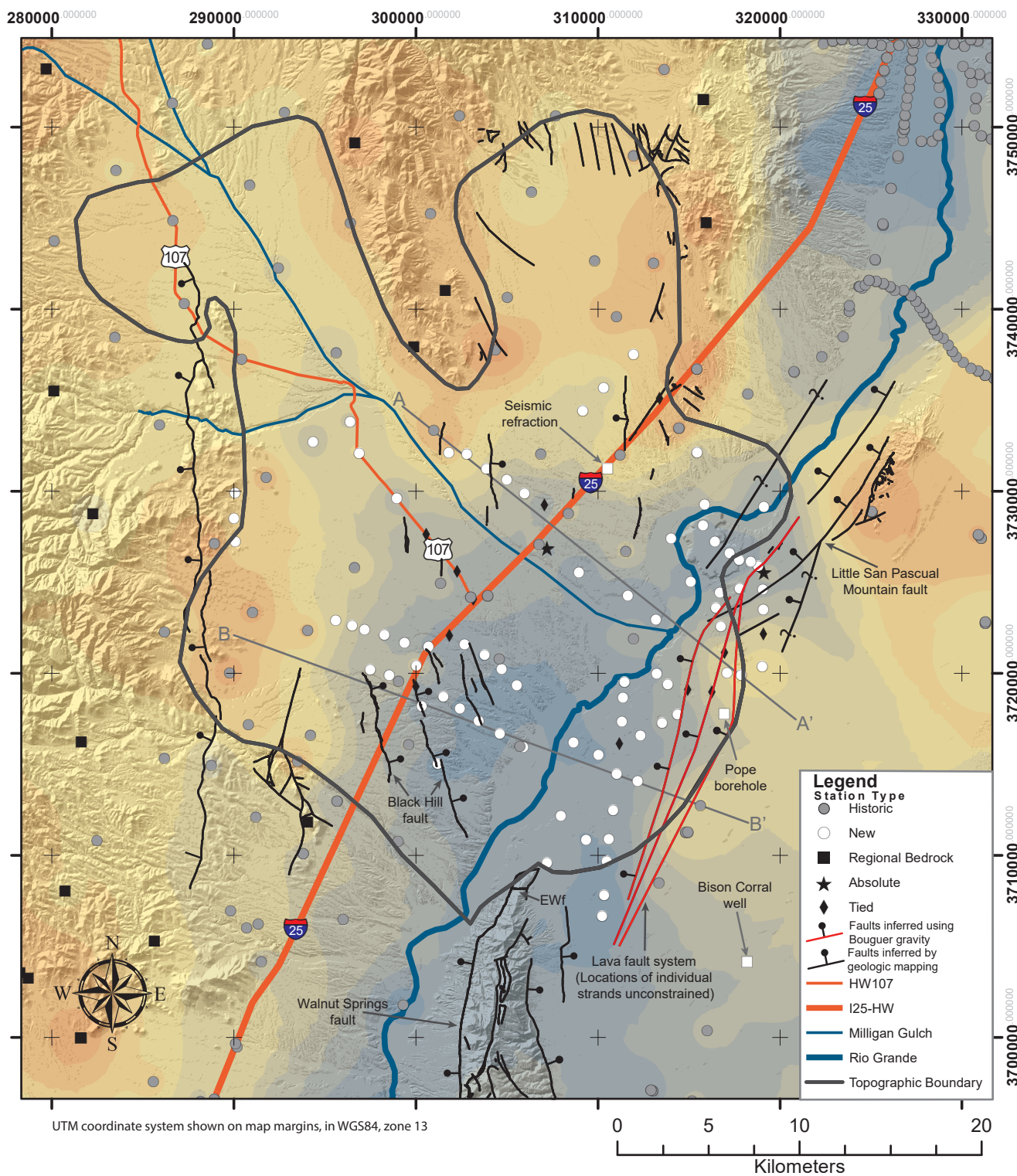


FIGURE 8. Residual map of total Bouguer anomalies. This map was made by subtracting the measured total Bouguer anomaly values from a regional bedrock trend approximated by a plane (decreasing to the west). Thirty-three stations on bedrock were used to fit a planar surface to their total Bouguer anomaly values using a least-squares regression in Matlab ($R^2 = 0.945$, residual mean of 10^{-13} mGal, standard deviation of 4.173 mGal, maximum absolute residual of 9.401 mGal). All bedrock stations are west of the Rio Grande and north of the Fra Cristobal Mountains (Fig. 5); residuals from the Rio Grande east are extrapolative.

Western Basin-Margin Structure (Black Hill Fault)

The western of these Bouguer gravity gradients is east-down and coincides with the mapped Black Hill fault (Figs. 7, 8). It separates the south-central gravity low from the aforementioned Bouguer anomaly high in the southwest corner of the San Marcial Basin. The gravity gradient is best defined where we have relatively abundant gravity data near its north-central section of the Black Hill fault. Inspection of the gravity profiles indicates an eastward drop of -20 mGals across the two strands of the Black Hill fault, which we have used to infer a doubling in the general thickness of the Santa Fe Group (Fig. 9). The fact that bedrock is mapped on the footwall of this fault (Fig. 3) is consistent with the interpretation that the gradient is due to a lateral juxtaposition of basin fill against bedrock due to faulting. Unfortunately, no deep wells are located on the hanging wall of this fault.

Eastern Basin Structure (Lava Fault Zone)

Our gravity data indicate a steep, west-down gradient 3–5 km east of where the Paraje Well fault was mapped by Koning et al. (2020b; Figs. 7, 8). We interpret that this gradient corresponds to a newly discovered west-down fault, which we call the Lava fault after the Lava siding on the Burlington Northern Santa Fe Railroad, and infer that this fault defines the eastern side of the San Marcial Basin. There is no evidence of a noteworthy west-down gravity gradient along the Paraje Well fault of Koning et al. (2020b), so we advocate querying or even deleting this fault from future geologic maps—perhaps to be reinstated if new drilling or geophysical data corroborates this structure.

The Bouguer anomaly and residual anomaly data show a westward decrease of 15–30 mGal across the Lava fault zone (Figs. 7–9). This gradient may be due to either west-tilted bedrock or to a ~ 2 km wide zone of faults that drop the bedrock floor of the basin down to the west. Near cross section B-B', we prefer a fault interpretation based on well data (see below) and the apparent offset at 25–26 km in the trend of the profiles of total Bouguer and residual gravity anomaly data (Fig. 9, B-B'). A homocline rather than a fault is permissible at the eastern end of profile A-A', based on a lack of a notable offset in the trend of west-sloping gravity profile data (Fig. 9). The eastern end of A-A' coincides with a slight westward bulge in both gravity maps (Figs. 7, 8) and may possibly represent a boundary zone between the Lava fault and the southern end of the Little San Pascual Mountains fault.

Unlike the Black Hill fault, no bedrock outcrops are found on the footwall of the Lava fault. However, the Bison Corral well and Pope borehole indicate the presence of shallow Cretaceous bedrock immediately east of the fault zone. The Bison Corral well is interpreted to penetrate shallow Cretaceous strata under a 15 m (50 ft) cover of Palomas Formation (Appendix 1). In contrast, the Pope borehole, interpreted to be located within the Lava fault zone, penetrated 91 m (400 ft) of Santa Fe Group and contains a 10 m (30 ft) thick gravel tongue within axial-fluvial sand; the texture and size of gravels in this tongue

suggest derivation from local paleotopographic bedrock highs to the east (Fig. 4; Kelley and Koning, this volume). Thus, independent geologic evidence offered by these two wells supports our interpretation that the Bouguer gradient here corresponds to a normal fault that has offset the top of the bedrock by at least 105 m (350 ft, derived from subtracting the 50 ft basin fill depth from the minimal bedrock depth of 400 ft at the Pope borehole), spatially corresponding (to within ~ 2 km) to where we have drawn the Lava fault zone (Figs. 3, 7, and 8).

DISCUSSION

Basin Geometry and Major Faults

The broad gravity low centered on the Rio Grande encompasses the south-central part of the San Marcial Basin. The low is bounded on the west by the northwest-striking Black Hill fault and on the east by the northeast-striking Lava fault and appears to narrow southwards towards the Engle Basin. The total Bouguer anomaly-low defining the basin floor becomes more negative westward toward the Black Hill fault (Figs. 7, 9). However, the residual anomaly appears to support a flatter, if still slightly deepening-to-the-west, basin bottom toward the Black Hill fault (Figs. 8, 9).

The residual gravity anomaly shows a possible extension of the San Marcial Basin northward toward the southern Socorro Basin, with a significant residual gravity low underlying Mesa del Contadero and the Rio Grande. We do not have sufficient data to define the northern boundary of this low-gravity “arm.” Nonetheless, after removing the regional trends, it appears that basin fill is thicker near Mesa del Contadero than seen solely by the Bouguer gravity anomaly.

The total Bouguer gravity anomaly map shows a large anomaly decrease near the northwestern corner of the topographic San Marcial Basin (Fig. 7). The San Mateo and Magdalena Mountains to the west and northwest of the main basin are composed of Eocene and Oligocene volcanics and are part of the northern edge of the Mogollon-Datil volcanic field; there is also an alignment of independently confirmed felsic calderas (from southwest to northeast): the Mount Withington, Hardy Ridge, and Socorro-Sawmill calderas (Fig. 7; Ferguson et al., 2012). Given these calderas, one could expect less dense crust and thus more negative Bouguer anomalies there. When the regional crustal trend is removed, we see that the residual anomaly shows thin to no basin fill in the northwest corner of the topographic San Marcial Basin (Fig. 8). This suggests that there is an extension of shallow–moderately thick basin fill of the San Marcial Basin northwest along NM State Route 107, but it does extend beyond 15 km northwest of the intersection of this road and I-25. In this extreme northwestern corner of the San Marcial Basin, the net effect on the gravity signal by the following features is poorly understood (compounded by the sparse gravity data coverage there): the interplay of tilted bedrock strata, poorly constrained normal faults, and the uncertain subsurface extent of possible low-density plutons underlying the aforementioned calderas.

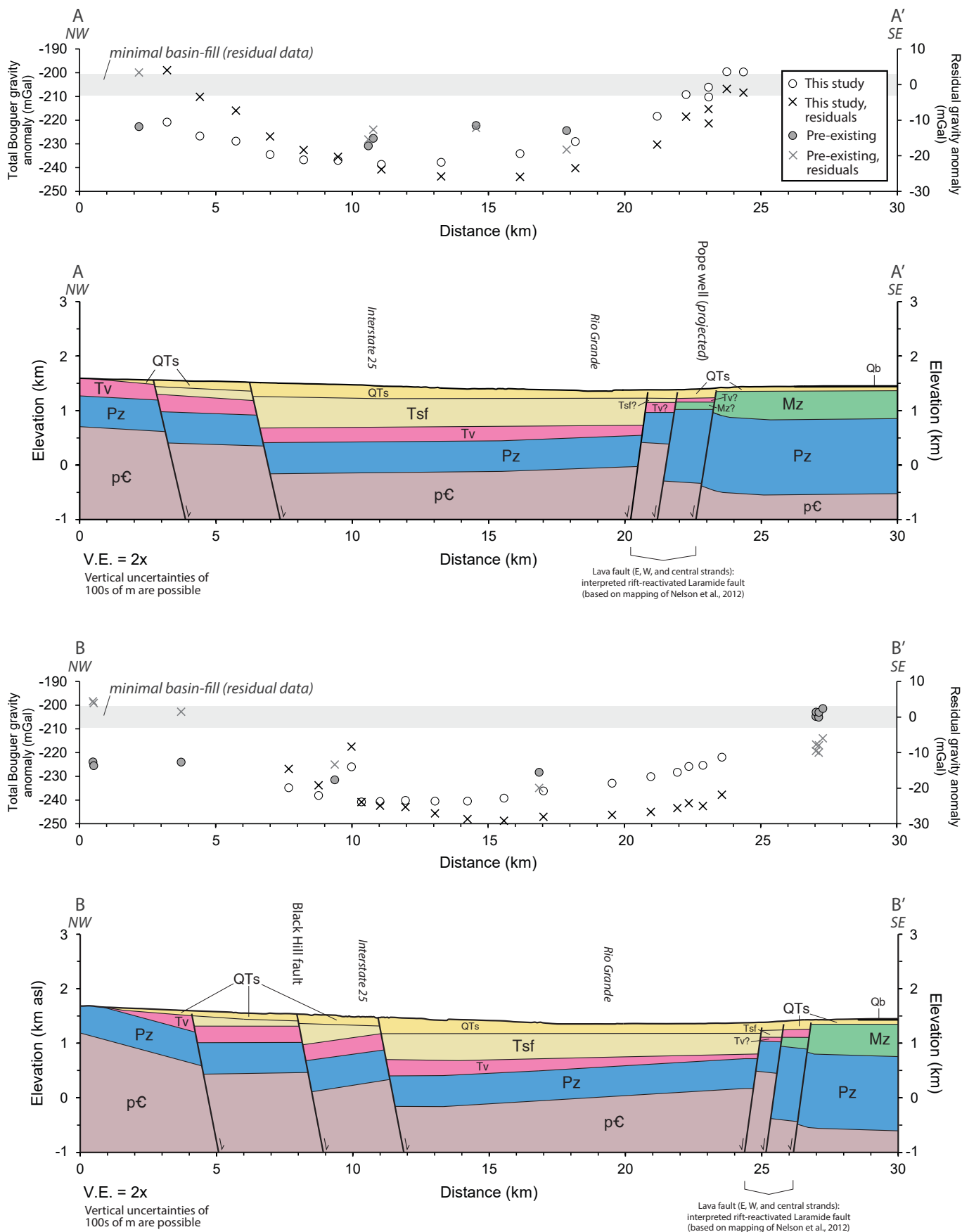


FIGURE 9. Cross sections A-A' and B-B' illustrating our inferred basin fill thickness variations and subsurface bedrock geology. Construction of these cross sections were guided by the profiles of total Bouguer and residual gravity anomaly values (Figs. 7, 8) that were projected orthogonally onto each line of section.

Structures Near the North End of the Fra Cristobal Mountains

The west-down Walnut Springs fault (Figs. 3, 7, and 8), was previously inferred to have continued to the northeast of the northern tip of the Fra Cristobal Mountains and serve as the basin-bounding fault (i.e., the Paraje Well fault of Koning et al., 2020b). Where the fault projects to the B-B' gravity profile (at km 23), however, there is no notable, west-down offset of the linear trend formed by the west-sloping gravity data. This suggests that there is no major-displacement, west-down fault here. Although, we acknowledge a fault could exist here, if it had relatively small offset of the top-of-bedrock or if it is an older structure juxtaposing basement types of similar densities. Because it was based solely on an assumption of fault continuity between the Walnut Springs fault and the Little San Pascual Mountain fault zone, we advocate querying or abandoning usage of the Paraje Well fault unless future data indicate otherwise. A Laramide reverse fault on the north end of the Fra Cristobal Mountains, juxtaposing Proterozoic rocks on the west against Pennsylvanian strata on the east (Fig. 3), likely continues approximately northeast from where it has been mapped previously (dotted fault southeast of the Paraje Well fault on Fig. 3). We note that there is an east-trending, north-down fault mapped 1 km south of the northern tip of the Fra Cristobal Mountains (labeled EWf in Figs. 7 and 8) that has juxtaposed Cretaceous strata against Proterozoic granite (Nelson et al., 2012; Lucas et al., 2019). Given the apparent absence of a northeast-striking gravity gradient coinciding with the northeastward projection of the Walnut Springs fault (i.e., the Paraje Well fault of Koning et al., 2020b), we suggest that a parallel east-west fault exists 1 km north of the labeled E-W fault, at the north end of the Cretaceous bedrock comprising the northernmost point of the Fra Cristobal Mountains. Both this fault and the western-bounding fault mapped by Nelson et al. (2012) may possibly link to the east-bounding fault of the Fra Cristobal Mountains (Fra Cristobal fault on Fig. 3).

The Bouguer and residual anomaly gradients defining the Lava fault continue southward past the north end of the Fra Cristobal Mountains, constrained by our new data and historical data (Figs. 7, 8), and also by the 15 m (50 ft) bedrock depth at the Bison Corral well. More data are needed southwest of our new data points, but our provisional interpretation is that the Lava fault bounds the east side of a narrow graben paralleling the east side of the Fra Cristobal Mountains. This graben would be bounded on the west by the Fra Cristobal fault and likely shallows to the south, based on subsurface interpretations to the south by Lozinsky (1987).

Thus, it is possible that the northern end of the Fra Cristobal Mountains is completely surrounded by extensional faults. The observation that the northern mountain block is east-tilted away from the main rift suggests that the highest vertical displacement occurs on the Walnut Springs fault, resulting in an east-dipping footwall uplift. Similar footwall uplifts of major basin-bounding faults that tilt away from the rift center are observed in many other places in New Mexico (e.g., Sandia, Oscura, Caballo, Sacramento, northern Magdalena, and Lemitar Mountains).

Lack of Topographic Expression of Footwall Uplift Boundary Faults

It is not clear why there is no topographic expression of a footwall uplift along the western and eastern bounding faults of the south-central San Marcial Basin, corresponding to the Black Hill and Lava faults, respectively. This is especially striking given the prominent footwall uplift (i.e., the east-dipping Fra Cristobal Mountains) on the Walnut Springs fault. One possible explanation is a higher density of crust on the footwalls of these two faults compared to that in the Fra Cristobal Mountains. Another hypothesis is a partitioning of strain northward from the Walnut Springs fault onto the Black Hill and Lava fault zones, resulting in a reduction of extensional strain on either of these northern faults compared to the Walnut Springs fault. The lower vertical displacements would reduce the amount of footwall unloading on these structures, resulting in lower uplift rates that could not outpace erosion and burial by late Cenozoic sedimentation. Future quantitative modeling is needed to test this partitioning hypothesis.

CONCLUSION

Synthesizing our 89 new data points with historical gravity data allows us to make inferences regarding the structure of the San Marcial Basin and qualitative assessments of basin fill thickness changes. Regionally, hypothesized low-density plutons underlying the vicinity of the northern San Mateo Mountains are provisionally observed in the total Bouguer anomaly, given that regional trend removal of crustal density variations caused these regions to have similar residual gravity anomalies; this argues for the San Marcial Basin gravity lows being associated with basin fill, not deeper structure. Based on maps of the total Bouguer anomaly, residual gravity anomaly, and two gravity profiles, we interpret a “main” Bouguer gravity anomaly low and residual gravity anomaly low between the Lava fault and the Black Hill fault, which likely corresponds to the area of deepest (thickest) clastic rift basin fill. A narrower “arm” of low-gravity anomalies suggest thick basin fill extends northeast of this main gravity low toward the Socorro Basin under Mesa del Contadero. Two other “arms” extend partly into the southern Highland Springs embayment and 15 km northwest of I-25 along Highway 107.

The Black Hill fault and the Lava fault are interpreted as the western and eastern bounding faults of the south-central San Marcial Basin. The southern end of the Lava fault appears to extend southward past the northern end of the Fra Cristobal Mountains. In a northward direction, extensional strain may possibly be partitioned from the north end of the Walnut Springs fault to the southern Black Hill fault and the Lava fault. This distribution of strain may result in each of these faults having less throw than the Walnut Springs fault. This partitioning may possibly explain the lack of a notable topographic expression of footwall uplift that might be expected to occur along these two faults, aside from scattered, small bedrock hills immediately west of the Black Hills fault. Future quantitative modeling is needed to test this strain-partitioning hypothesis.

ACKNOWLEDGMENTS

We thank the reviewers, Ben Drenth and Tien Grauch, for their helpful comments, which substantially improved the quality of this paper. Gallant was funded by the New Mexico Bureau of Geology's Bright Star Program and New Mexico Tech E&ES department funds. R. David Wheeler of the Department of Defense contributed to general survey methods. The Bureau of Land Management and all private landowners who allowed access to new areas for the survey are also thanked for their willingness and accommodation. The authors of this paper would also like to thank several students that contributed in conversation and fieldwork for the survey, including Samuel Otu, Ethan Williams, Alexandra Sartori, David Cavazos, Xavier Romero, and Daniel Dolce.

REFERENCES

- Adams, D.C., and Keller, G.R., 1994, Crustal structure and basin geometry in south-central New Mexico, *in* Keller, G.R., and Cather, S.M., eds., Basins of the Rio Grande Rift: Structure, Stratigraphy, and Tectonic Setting: Boulder, Colorado, Geological Society of America, Special Paper 291, p. 241–255.
- Biehler, S., Ferguson, J., Baldrige, W.S., Jiracek, G.R., Aldren, J.L., Martinez, M., Fernandez, R., Romo, J., Gilpin, B., Braile, L.W., Hersey, D.R., Luyendyk, B.P., and Aiken, C.L., 1991, A geophysical model of the Española basin, Rio Grande rift, New Mexico: *Geophysics*, v. 56, p. 340–353.
- Chamberlin, R.M., McIntosh, W.C., and Eggleston, T.L., 2004, ⁴⁰Ar/³⁹Ar geochronology and eruptive history of the eastern sector of the Oligocene Socorro caldera, central Rio Grande rift, New Mexico: New Mexico Bureau of Geology and Mineral Resources, Bulletin 160, p. 251–253.
- Chapin, C.E., 1979, Evolution of the Rio Grande rift – a summary, *in* Riecker, R.E., ed., Rio Grande Rift, tectonics and magmatism: Washington, D.C., American Geophysical Union, p. 1–5.
- Chapin, C.E., and Cather, S.M., 1994, Tectonic setting of the axial basins of the northern and central Rio Grande rift, *in* Keller, G.R., and Cather, S.M., eds., Basins of the Rio Grande Rift: Structure, Stratigraphy, and Tectonic Setting: Boulder, Colorado, Geological Society of America, Special Paper 291, p. 5–25.
- Cikoski, C.T., Roth, S.J., and Osburn, G.R., 2013, Geologic map of the Cienga Ranch quadrangle, Socorro County, New Mexico: New Mexico Bureau of Geology and Mineral Resources, Open-file Digital Geologic Map 239, scale 1:24,000.
- Connell, S.D., 2008, Geologic map of the Albuquerque-Rio Rancho metropolitan area and vicinity, Bernalillo and Sandoval Counties, New Mexico: New Mexico Bureau of Geology and Mineral Resources, Geologic Map 78, 1:200,000.
- Connell, S.D., Smith, G.A., Geissman, J.W., and McIntosh, W.C., 2013, Climatic controls on nonmarine depositional sequences in the Albuquerque Basin, Rio Grande rift, north-central New Mexico, *in* Hudson, M.R., and Grauch, V.J.S., eds., New Perspectives on Rio Grande Rift Basins: From Tectonics to Groundwater: Geological Society of America, Special Paper 494, p. 383–425, doi: 10.1130/2013.2494(15).
- Deal, E.G., 1973, Geology of the northern part of the San Mateo Mountains, Socorro County, New Mexico: as study of a rhyolite ash-flow tuff cauldron and the role of laminar flow in ash-flow tuffs [Ph.D. dissertation]: Albuquerque, University of New Mexico, 268 p.
- Deal, E.G., and Rhodes, R.C., 1976, Volcano-tectonic structures in the San Mateo Mountains: New Mexico Geological Society, Special Publication 5, p. 51–56.
- Donze, M.A., 1980, Geology of the Squaw Peak area, Magdalena Mountains, Socorro County, New Mexico: New Mexico Bureau of Mines and Mineral Resources, Open-file Report 123, 131 p.
- Drenth, B.J., Grauch, V.J.S., Turner, K.J., Rodriguez, B.D., Thompson, R.A., and Bauer, P.W., 2019, A shallow rift basin segmented in space and time: The southern San Luis Basin, Rio Grande rift, northern New Mexico, U.S.A.: *Rocky Mountain Geology*, v. 54, no. 2, p. 97–131, <https://doi.org/10.24872/rmgjournal.54.2.97>.
- Ferguson, C.A., 1986, Geology of the east-central San Mateo Mountains, Socorro County, New Mexico: New Mexico Bureau of Mines and Mineral Resources, Open-file Report 252, 124 p.
- Ferguson, C.A., 1990, Geology of the Grassy Lookout 7.5-minute quadrangle, Socorro County, New Mexico: New Mexico Bureau of Mines and Mineral Resources, Open-file Report 366, 38 p.
- Ferguson, C.A., 1991, Stratigraphic and structural studies in the Mt. Withington Cauldron, Grassy Lookout quadrangle, Socorro County, New Mexico: *New Mexico Geology*, v. 13, p. 50–54.
- Ferguson, C.A., and Osburn, G.R., 1994, Geology of the Mt. Withington 7.5-minute quadrangle, Socorro County, New Mexico: New Mexico Bureau of Mines and Mineral Resources, Open-file Report 403, scale 1:24,000.
- Ferguson, C.A., Osburn, G.R., and McIntosh, W.C., 2012, Oligocene calderas in the San Mateo Mountains, Mogollon-Datil volcanic field, New Mexico: *New Mexico Geological Society, Guidebook 63*, p. 74–77.
- Gilmer, A.L., Mauldin, R.A., and Keller, G.R., 1986, A gravity study of the Jornada del Muerto and Palomas basins, *in* Clemons, R.E., King, W.E., Mack, G.H., and Zidek, J., eds., Truth or Consequences region: New Mexico Geological Society, Guidebook 37, p. 131–134.
- Grauch, V.J.S., and Connell, S.D., 2013, New Perspectives on the geometry of the Albuquerque Basin, Rio Grande rift, New Mexico: Insights from geophysical models of rift-fill thickness, *in* Hudson, M.R., and Grauch, V.J.S., eds., New Perspectives on Rio Grande Rift Basins: From Tectonics to Groundwater: Geological Society of America, Special Paper 494, p. 427–462, doi: 10.1130/2013.2494(16).
- Grauch, V.J.S., Phillips, J.D., Koning, D.J., Johnson, P.S., and Bankey, V., 2009, Geophysical interpretations of the southern Española Basin, New Mexico, that contribute to understanding its hydrogeologic framework: *U.S. Geological Survey, Professional Paper 1761*, 88 p.
- Grauch, V.J.S., Bauer, P.W., Drenth, B.J., and Kelson, K.I., 2017, A shifting rift – geophysical insights into the evolution of Rio Grande rift margins and Embudo transfer zone near Taos, New Mexico: *Geosphere*, v. 13, p. 870–910.
- Haneberg, W.C., Reynolds, C.B., and Reynolds, I.B., 1991, Geophysical characterization of soil deformation associated with earth fissures near San Marcial and Deming, New Mexico, *in* Land Subsidence, Proceedings of the Fourth International Symposium on Land Subsidence, May: LAHS Publ. no. 200, p. 271–280.
- Hinze, W.J., Von Frese, R.R.B., and Saad, A.H., 2013, Gravity and Magnetic Exploration: Principles, Practices, and Applications: New York, Cambridge University Press, doi:10.1017/CBO9780511843129.
- Hirt, C., Yang, M., Kuhn, N., Bucha, B., Kurzmann, A., and Pail, R., 2019, SRTM2: An Ultrahigh Resolution Global Model of Gravimetric Terrain Correction: *Geophysical Research Letters*, v. 46, p. 4618–4627.
- Jochems, A.P., and Koning, D.J., 2019, Geologic map of the Black Hill 7.5-minute Quadrangle, Socorro County, New Mexico: New Mexico Bureau of Geology and Mineral Resources, Open-File Geologic Map 274, scale 1:24,000.
- Kelley, S.A., and Koning, D.J., this volume, Audio-magnetotelluric survey of a shallow aquifer east of Mesa del Contadero, central New Mexico: *New Mexico Geological Society, Guidebook 72*.
- Kluth, C.F., and Schaftenaar, C.H., 1994, Depth and geometry of the northern Rio Grande rift in the San Luis Basin, south-central Colorado, *in* Keller, G.R., and Cather, S.M., eds., Basins of the Rio Grande rift: Structure, stratigraphy, and tectonic setting: Boulder, Colorado, Geological Society of America, Special Paper 291, p. 27–37.
- Koning, D.J., this volume, How geology and topography influenced the Battle of Valverde (February 21, 1862): *New Mexico Geological Society, Guidebook 72*.
- Koning, D.J., Grauch, V.J.S., Connell, S.D., Ferguson, J., McIntosh, W., Slate, J.L., Wan, E., and Baldrige, W.S., 2013, Structure and tectonic evolution of the eastern Española Basin, Rio Grande rift, north-central New Mexico, *in* Hudson, M., and Grauch, V.J.S., eds., New Perspectives on the Rio Grande rift: From Tectonics to Groundwater: Geological Society of America, Special Paper 494, p. 185–219, doi:10.1130/2013.2494(08).

- Koning, D.J., Pearthree, K.S., Jochems, A.P., and Love, D.W., 2020a, Geologic map of the San Marcial 7.5-minute quadrangle, Socorro County, New Mexico: New Mexico Bureau of Geology and Mineral Resources, Open-file Geologic Map 287, scale 1:24,000.
- Koning, D.J., Jochems, A.P., Hobbs, K.M., Pearthree, K.S., and Love, D.W., 2020b, Geologic map of the Paraje Well 7.5-minute quadrangle, Socorro County, New Mexico: New Mexico Bureau of Geology and Mineral Resources, Open-file Geologic Map 286, scale 1:24,000.
- Koning, D.J., Hobbs, K.M., Pearthree, K.S., and Love, D.W., 2021, Geologic map of the Fort Craig 7.5-minute quadrangle, Socorro County, New Mexico: New Mexico Bureau of Geology and Mineral Resources, Open-file Geologic Map 288, scale 1:24,000.
- Longman, I.M., 1959, Formulas for computing the tidal accelerations due to the moon and the sun: *Journal of Geophysical Research*, v. 64, p. 2351–2355.
- Lozinsky, R.P., 1987, Cross section across the Jornada del Muerto, Engle, and northern Palomas Basins, south-central New Mexico: *New Mexico Geology*, v. 9, no. 3, p. 55–57, 63.
- Lucas, S.G., Nelson, W.J., Krainer, K., and Elrick, S.D., 2019, The Cretaceous system in central Sierra County, New Mexico: *New Mexico Geology*, v. 41, no. 1, p. 3–39.
- Machette, M.N., and Jochems, A.P., compilers, 2016a, Fault number 2102, Walnut Springs fault, *in* Quaternary fault and fold database of the United States: U.S. Geological Survey website, <https://earthquakes.usgs.gov/hazards/qfaults> (accessed 03/30/22).
- Machette, M.N., and Jochems, A.P., compilers, 2016b, Fault number 2130, Black Hill fault, *in* Quaternary fault and fold database of the United States: U.S. Geological Survey website, <https://earthquakes.usgs.gov/hazards/qfaults> (accessed 03/30/22).
- Morgan, G.S., Koning, D.J., Shackley, M.S., Love, D.W., Hobbs, K.M., and Jochems, A.P., this volume, Early Pleistocene (late Blancan) vertebrates from Simon Canyon, Socorro County, central New Mexico: *New Mexico Geological Society, Guidebook 72*.
- Nelson, E.P., 1986, Geology of the Fra Cristobal Range, south-central New Mexico: *New Mexico Geological Society, Guidebook 37*, p. 83–91.
- Nelson, W.J., Lucas, S.G., Krainer, K., McLemore, V.T., and Elrick, S., 2012, Geology of the Fra Cristobal Mountains, New Mexico: *New Mexico Geological Society, Guidebook 63*, p. 195–209.
- NMBGMR [New Mexico Bureau of Geology and Mineral Resources], 2003, Geologic Map of New Mexico: New Mexico Bureau of Geology and Mineral Resources, scale 1:500,000.
- Sion, B.D., Phillips, F.M., Axen, G.J., Harrison, B.J., Love, D.W., and Zimmerer, M.J., 2020, Chronology of terraces in the Rio Grande rift, Socorro basin, New Mexico: Implications for terrace formation: *Geosphere*, v. 16, p. 1–23, <https://doi.org/10.1130/GES02220.1>.

Appendices can be found at

<https://nmgs.nmt.edu/repository/index.cfm?rid=2022004>